Bulgarian Chemical Communications, Volume 52, Issue 1 (pp. 29-46) 2020 DOI: 10.34049/bcc.52.1.4942

Mechanical analysis of additively manufactured polylactic acid in fused deposition modelling

A. Mushtaq[1]*, A. Israr[1], M. Fahad[2], J. Ahmed[1]

[1]*Polymer and Petrochemical Engineering Department,*
[2]*Industrial Manufacturing Department, NED University of Engineering & Technology, Karachi, Sindh, Pakistan*

Received September 8, 2018, Revised August 19, 2019

Additive manufacturing technology is a most widely used technique to manufacture 3D printed objects by adding layer over layer of specific material. Additive manufacturing referred physical fabrication of 3D model by accumulating many layers of different materials, providing vast flexibility in physical structure and geometry. This study focused on Fused Deposition Model (FDM) that will help to analyze two basic parameters (raster angle and number of contours) of 3D model objects to determine the tensile strength of different specimen made from polylactic acid (PLA) having a constant infill density of 25%. The part build with concentric pattern shows the highest tensile strength with number of contours 2, 3 and 4. With the mathematical models for four different raster angles there is a better understanding of how the FDM manufactured objects of PLA material would behave under loading.

Keywords: 3D printing; Additive manufacturing; Fused Deposition Modelling; Polylactic acid.

INTRODUCTION

According to ASTM international committee (F 42), additive manufacturing technology is defined as "the process of joining material to make an object from three-dimensional (3D) model data usually layer by layer as opposed to substrate manufacturing methodology" [1]. Additive manufacturing (AM) is a computer-assisted process that helps in the physical fabrication of 3D objects using metals, plastics, ceramics, compost and biological material, deposited layer over layer and forming a 3D structure. Additive manufacturing is an effective reverse engineering technique that helps in redesigning and manipulating a product that already exists [2]. The concept of additive manufacturing, also known as 3D printing, rapid prototyping and solid free form was developed in the early 1980s by Charles Hull. In 1986 Hull developed a 3D system under the name of stereolithography (STL), in which he established a format of STL file with the help of computer-aided design (CAD) software to get a 3D object printed [3]. After the inception of assistive manufacturing in the mid-1980s, the technology has evolved, so much that a number of different methodologies have been discovered.

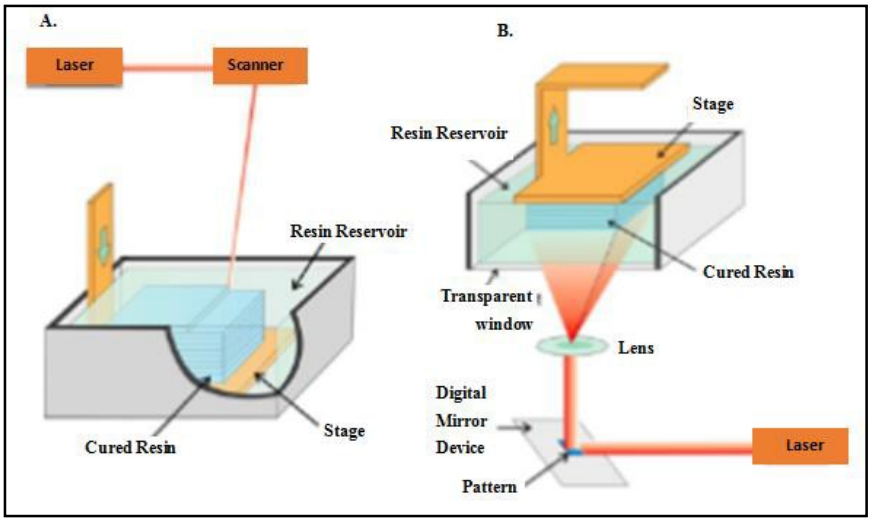

Fig. 1. Schematic of stereolithography

* To whom all correspondence should be sent:
E-mail: engrasimmushtaq@yahoo.com

The major additive manufacturing processes are stereolithography, fused deposition modelling (FDM), inkjet printing, selective laser sintering, 3D printing, laminated object manufacturing and laser metal deposition [1].

Hull invented in 1986 the first additive manufacturing process named stereolithography. It was the first AM technique used commercially by 3D System Inc. [3]. Stereolithography is an additive manufacturing (AM) technique which is used to fabricate a complete 3D structure of a plastic monomer using computer-aided design (CAD) data by different binding layers of photopolymers under the process of photo polymerization [4].

In Figure 1 the process of stereolithography initiates when a spot beam of ultra violet (UV) light moves across the surface of curable plastic monomer. The incident UV light initiates the polymerization reaction across the surface of the liquid monomer and start solidifying. Once a layer of solidified material with a required thickness is formed the solid material is taken below the liquid surface and new liquid monomer, in turn, starts to solidify under programmed manner. The newly formed layer then immediately adheres to the preceding layer. The process continues until the 3D object is completely formed [4].

UV curable resins, waxes and ceramics are extensively used in stereolithography [3]. Fused Deposition Model is the most widely additive manufacturing technique. It was developed by Scott Crump in 1989. The technique was patented by Stratasys [3]. The most common additive manufacturing technique is fused deposition modelling (FDM). In FDM process the first step is to generate the 3D model of the part using computer aid design (CAD).

The model is then exported to FDM machine software where it converts the design into basic components of a 2D small triangular structure. This information is further used in the physical generation of the model [3, 5]. Once a 3d model is formed in CAD software, a molten state thermoplastic is extruded form the machine and deposits layer over layer forming a 3 D structure [3].

Thermoplastics and waxes can be used in FDM machines as shown in Figure 2. Selective laser sintering (SLS) techniques were invented by Deckard and Beaman in 1980 [3]. Selective laser sintering (SLS) is a technique used in additive manufacturing. The process involves manufacturing of 3D object by using powder material that selectively fuses by laser radiation and deposits layer over layer to form a three-dimensional product. The laser radiation helps to initiate the process by partially melting the product; the liquid form by molten material binds the surrounding powder, solidifies and consolidates once the temperature decreases [6-8].

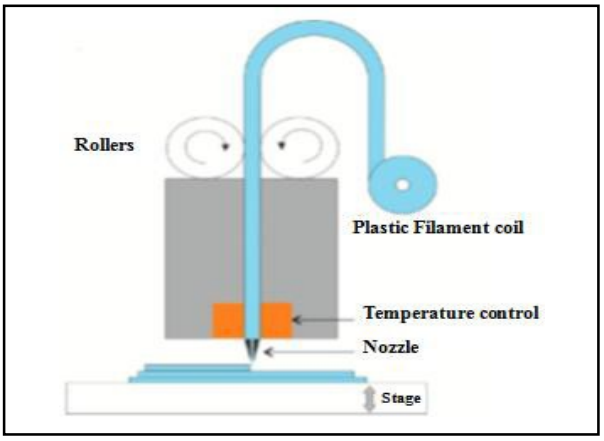

Fig. 2. Schematic of fused deposition model [3].

In a laser sintering process the powder material is sintered selectively by a laser beam to produce an initial sintered layer of specific dimensions as shown in Figure 3. The first formed sintered layer corresponds to the initial structure of the desired product. The sintering process continues until a three-dimensional structure with a specific design is formed. The laser beam in the sintering process helps to selectively sinter the powder material with specific boundaries and desired structure [6]. Thermoplastics and metals can be used in SLS.

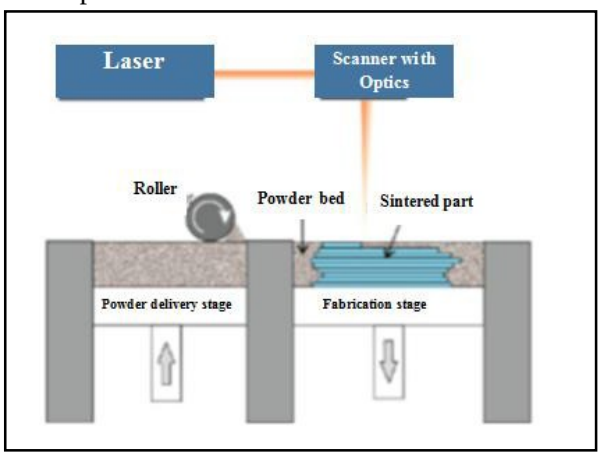

Fig. 3. Schematic of selective laser sintering [3].

The initial concept of the inkjet printer was developed in 1878 by Lord Rayleigh. In 1951, Siemens patented the 2D inkjet type printer called “Rayleigh breakup inkjet device” as shown in Figure 4. Inkjet printing is a powder-based 3D manufacturing process. In inkjet printing, the powder material is bound together by printing liquid that helps in binding the powder and results in the formation of a 3D structure [3].

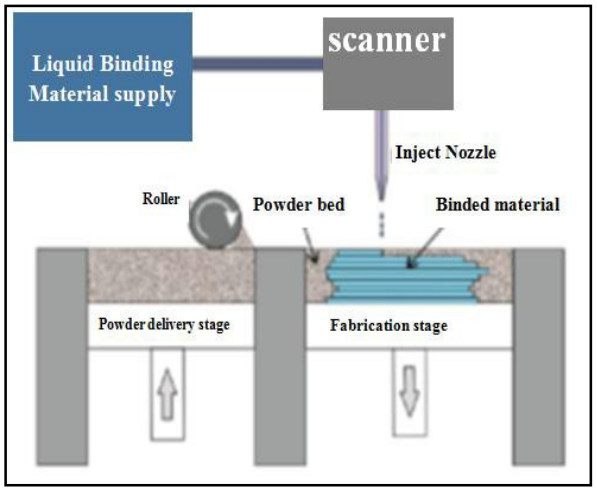

Fig. 4. Schematic of inkjet printing.

A layer of evenly distributed powder material was formed with the help of rollers which form the initial stage of the inkjet process. Once a layer is formed, the printer drops binding liquid material onto the powder making a specific shape. After the completion of the first stage, the second layer of powder is distributed and selectively binds with the initial layer of material. The process is repeatedly performed until a 3D structure is formed. Once the desired product is formed the model is heated to enhance the binding strength between the layers. Unlike other 3 D processses, inkjet printing has an edge of providing support material in terms of unbound powder material which can be reused after the material is printed [3, 9]. Composites, polymer-ceramics and metals are used for inkjet printers.

All discussed techniques are being used in the rapid prototyping for the production of consumer end product. 3D Systems Inc. and Stratasys Inc. have acquired the largest market share in 3D prototyping due to their modern technique.

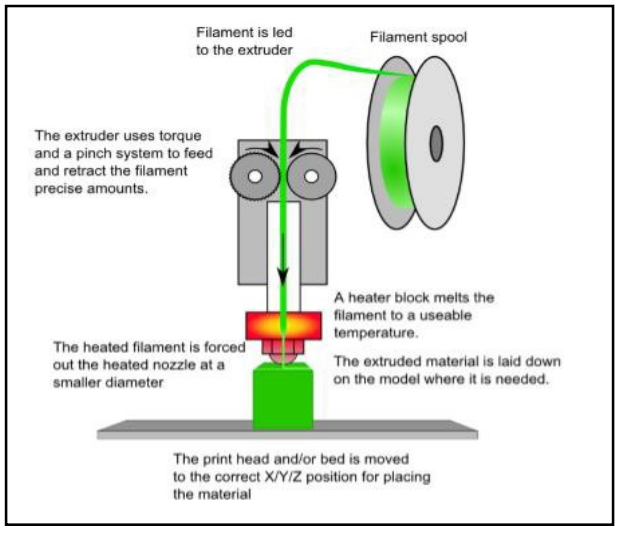

Fig. 5. Schematic of Fused Deposition Modelling [11].

Literature Review

Fused deposition modelling (FDM) is the most popular additive manufacturing technique that produces a physically fabricated model using computer-aided deign. The FDM technology is patented by Stratasys Inc. This technology basically relies on the robotic arm with a head which extrudes the melted thermoplastic filament. Stratasys first sold their machine in 1992 by the name of 3D modeller. The early product of the company could replicate different 3D models. However, the machine was not able the take big markets to share due to its low volume productivity so in 1993 Stratasys introduced its second product by the name of "The Benchtop", which was roughly the size of a refrigerator. The machine not only has the ability to deal with high volume but is also suitable to manufacture industrial-scale prototype [10].

In the mid 1980's IBM developed a small 3D printer that works on an extrusion system similar to that of Stratasys. The major difference between the two products was the feeding system. In 1995 Stratasys offered IBM to co-develop a 3D printer which resulted in the introduction of "the Genisys" 3D printer. The product found an overwhelming response of market in its first year. However, it faced a number of major problems including the contaminant wafer that could not melt properly at the operating temperature, leaving small particles that jammed the nozzles. It also has a drawback that once the model gets cooled it has the tendency to curl along the edges. In 1998 after selling 130 units, Stratasys stopped the production of Genisys, and returned the product with the name of "Genisys Xs" [10].

In 1997 Stratasys got the clearance from the department of food and drug administration and started working in the field of medicine. They introduced their "Med Modeler" system which was specifically designed to serve in the field of medicine by producing anatomical parts for MRI and CT scan [10]. Stratasys further introduced its product named "FDM Quantum" that offers a large envelope for an additive manufacturing system. The product offers a proper networking system which enables a number of uses to work together [10]. In 2000, Stratasys introduced "prodigy" which was capable of making sample typed 8×8×12 inches with three different layer thicknesses. In late 2000, Stratasys released "FDM Maxum" with a big envelop modeller and water work support which reduces the processing time by reducing the post-processing work by clean prototype [10]. The product replaced the IBM wafer system by a plastic filament that was fed in the nozzle by heating the

material to its melting temperature, as shown in Figure 5.

This not only simplified the process but also reduced the manufacturing time by adopting a simple mechanism. With the introduction of "dimension". Stratasys regained his market share, a month further after the introduction of "dimension", Stratasys presented his new products named "Prodigy Pus" and "FDM Vintage" [10]. In 2004 Stratasys introduced "Dimension SST", which was capable of producing complex models and prototypes [10]. The main components of the FDM machine are the nozzle or the liquid head, the axes, the building envelope and the controller. There is a number of thermoplastic materials which can be used in the FDM machine. Acrylonitrile butadiene-styrene (ABS) is the most commonly used material in FDM [5]. However, in recent advancement in the field of 3D printing, high advanced material such as ULTEM^{TM} 9085 resin can also be incorporated in FDM machines [12, 13]. With the emergence of Open source 3D printer polylactic acid is the most widely used material in printers due to its vast durability and low processing temperature [5].

Recent advancement in the field of the polymer has paid much attention to a biodegradable polymer. Polylactic acid is the most widely used material in 3D printing that is a linear aliphatic thermoplastic degrading biologically. The thermal stability of polylactic acid was studied by F. Carrasco who explained that using TGA data at low processing temperature the amount of fumes released from the sample is of very less amount which makes it environmentally friendly [14]. The mesostructure of polylactic acid explains that due to the small methyl group linked with the main C-C chain, the chain can easily slide making it easy to extrude the material; hence it is easy to process. The melt flow index (MFI) lies in the range of 7g/10 min to 10.7g/10 min depending upon the crystallinity of PLA .which shows that there is a linear relation between the chain alignment and MFI.

Similarly, if we compare polylactic acid with acrylonitrile butadiene (ABS) it is witnessed that due to the high melting point the deposited layer deforms due to high- temperature gradient which makes it difficult to process. It is also shown that the temperature distribution in the fiber is highly non-uniform due to which the building structure deforms [15]. The melting point of acrylonitrile butadiene nitrile (ABS) is around 230 ^{o}C at which the fumes released consist of phenols, styrene and butadiene, which make the environment unsafe when printing [16].

FDM process deals with a number of parameters that need control for optimizing the process. The selection of parameters solely depends on the application of a product which is being manufactured. The control parameters likely affect the mechanical properties, final finish and processing temperature of the part. The final parameters that could affect the final product processing by FDM technology are build orientation, nozzle and bed temperature, layer thickness, contour (vertical shells), infill density, raster angle and horizontal shell [17]. The build orientation of FDM manufactured pat refers to the direction of beads of material concerning the loading of the part. At first, the specimen is configured to which axis it is geometrically built [18].

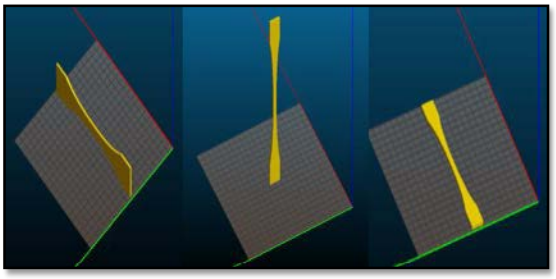

Fig. 6. Build orientation at x, y and z-direction

The built specimen can be in the direction of x, y and z-axis, as shown in Fig. 6. However, all three build directions have a different effect on the mechanical properties of the sample. Figure 6 shows the build orientation of different samples; the first picture shows the building of sample at x direction, similarly the other two pictures show the build orientation at y and z-direction, respectively. A further illustration of different orientations concerning different build angle is shown in Figure 7. With every different orientation, the tensile strength varies depending upon the filaments alignment, applied force and build pattern.

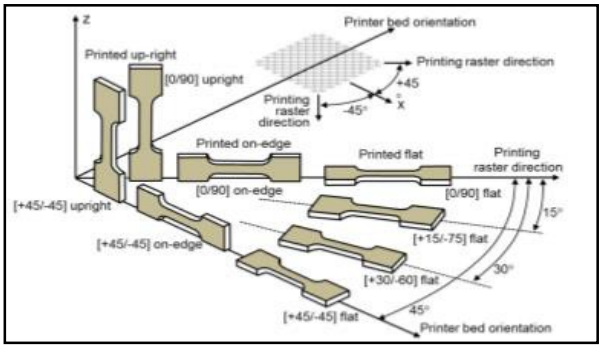

Fig. 7. Sample built with different raster angles and build orientation [19].

Nozzle and bed temperature

The selection of nozzle and bed temperature is a function of the material used. Typically for PLA the

nozzle temperature ranges from 200 to 210 ºC and bed temperature could be in the range of 0-60 ºC.

Layer thickness

The layer thickness is the amount of material that could be deposited from the nozzle. The amount of material is determined by the nozzle diameter. The layer thickness also depends upon the feed rate of the machine. At maximum feed rate, the deposited layer shows consistency in diameter, hence shows constant layer thickness.

Contour (number of shells)

After build orientation, the number of contouring is the major factor that determines the properties of the sample. A number of contours determine the outer layer thickness of the sample. The higher the number of the layers the more finished manufactured model will be. In Figure 8 the samples are built with a number of outer perimeters 4 and 1, respectively. The number of the contours can vary depending upon the layer thickness and build pattern.

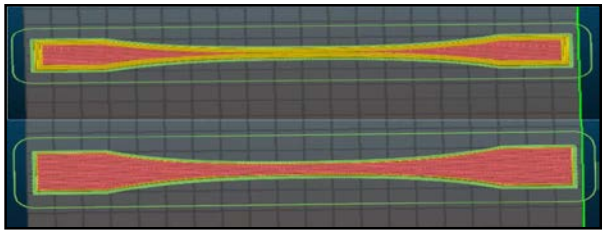

Fig. 8. Samples with number of contours 4 (top) and 1 (bottom).

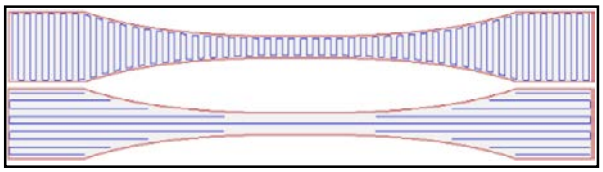

Fig. 9. Samples with infill density of 100% and raster orientation 0º.

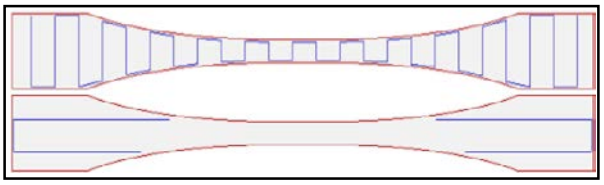

Fig. 10. Samples with infill density of 25% and raster orientation 0 º.

Infill density

Infill density refers to the distance between two layers. The larger the gap between the layers, less dense is the sample at short processing time. Although a sample with no gap between the layers is denser at a longer processing time. The infill density ranges from 0 to 100 % as shown in Figure 9.

The above figure illustrates that the higher the infill density, the denser the sample would be, but the effect of infill density on tensile strength decreases after reaching the point where tensile strength is maximum as shown in Figure 10.

Raster angle

Raster angle is the direction at which the bead of material moves relative to the direction at which part is loaded. The value of raster angle ranges from 0 º to 45 º.

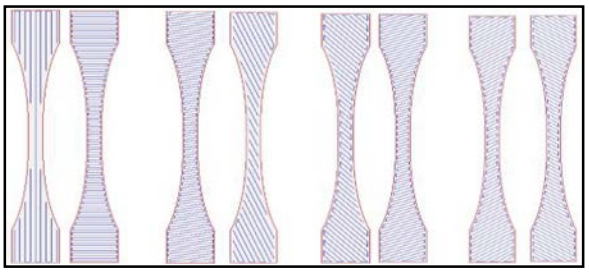

Fig. 11. Raster angle: (i) 0º, (ii) 15º, (iii) 30º and (iv) 45º.

Figure 11 shows the build pattern of different samples made with the raster angle 0º, 15º, 30º and 45º, respectively. Similarly, figure 12 shows that besides build pattern with a certain angle the sample can be made using build pattern of concentric and honey comb structure.

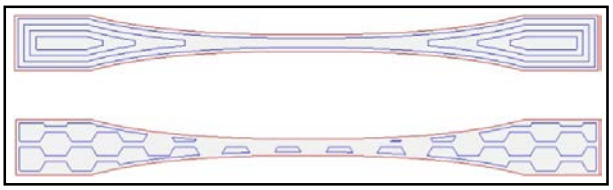

Fig. 12. Fill pattern: concentric (top) and honey comb (bottom)

Horizontal shells

Horizontal layers refer to the extreme top and bottom layers having the infill density of 100%. The solid top and bottom layers of the fabricated part help enhancing the finish and tensile strength of the final product.

Speed

The speed of the deposited material is determined by the OEM. However, with maximum build speed the time to fabricate a material decreases. Process parameters are some of the key factors that determine the quality and the strength of the finished good. A number of process parameters can be varied so that their influence can be studied on the final manufactured good. Various

design, methods and strategies have been studied to assist the manufacturing process of prototyping.

Es-Said *et al*. examined the tensile strength of an ABS sample with different layer orientations indicating the relation of yield and ultimate strength with orientation [20]. Experimental data collected were analyzed by a three-point methodology which illustrated that modulus of rapture is greater when the sample layers are oriented at 0°. However, the value decreases when the layer orientation is 90°, this is because the FDM sample has weak interlayer bonding or porosity. He also concluded that due to different layer deposition the overall sample exhibits an anisotropic characteristic. Since the sample shows an anisotropic property, the layer orientation with a different angle (e.g. 45° /-45°, 0° /45°, 90°) has a significant effect on the tensile strength. Therefore it can be concluded that anisotropy is affected by the angle at which the sample is produced depending upon the porosity and layer orientation.

Montero *et al.* have found that the physical parameters of FDM sample (i.e. air gap and raster orientation) had great effect on the tensile strength of parts, however, temperature has little effect [21]. The investigation showed that tensile strength of the part produced by crisscross orientation (45°/-45°) shows isotropic characteristics. It was noticed that axial orientation is higher as compared to transverse orientation. The crisscross orientation with zero elastic module is higher as compared to the negative air gap. The stress-strain curve of the sample produced when layers are axially oriented revealed that with an increase in the percentage of strain the stress increases reaching to a point after which the percentage change in strain has little effect on stress, however the stress-strain curve in transverse raster orientation exhibits brittle behavior.

Ahn *et al.* have comparatively analyzed the tensile strength of an ABS sample produced by FDM and an ABS sample produced by injection moulding process [18]. The FDM sample was fabricated with 12 layers with different raster angles and having a certain air gap. The investigation of the results showed that the sample produced with raster angle 0°/0° and 0°/90° had higher tensile strength as compared to a sample produced with the crisscross orientation of raster angle 45°/-45°. However, the sample oriented at the angle of 90° showed the least value of tensile strength as compared to the sample produced by injection molding. This magnifies the results that in the axial direction 0° the gap in-between the fibres decreases the effective cross-sectional area whereas in a transverse direction 90° the tensile load is distributed only on the bond, not on the fibres, hence showing a lower tensile strength. The crisscross specimen shows a shear failure at the angle of 45° which is because of the repetitive application of tension and shear force.

Sun *et al*. conducted experiments in which the relation between process conditions and quantity of layer formed in FDM processed parts was studied [22, 23]. The findings were based on the neck formation between the two deposited layers and the failure under the application of flexural load. The result concluded that as regards the flexural strength, the temperature has great influence on FDM parts. The further results showed that the temperature of the bottom layer of the FDM parts remains higher than the glass transition temperature over a longer period of time. As the number of the deposited layer increases, the phenomenon of stress generation due to greater temperature gradient is more prominent. A study conducted by Sood *et al*. showed the relation between tensile strength and layer thickness, part build orientation, raster angle, raster to raster gap and raster width [17]. The parts were fabricated using FDM, and experimental data were collected by forced centered central design (FCCD) run where the contour width was kept constant at the value of 0.4064 mm. The results showed that tensile strength and flexural strength of a sample fabricated using ISO R527:1966 can be significantly affected by the physical processing properties.

In a three-point analysis process where the range of layer thickness was from 0.1270 mm to 0.2540 mm, raster angle from 0 ° to 60 °, raster width from 0.04064 mm to 0.5064 mm and air gap from 0.00 mm to 0.0080 mm, the investigation results showed that the tensile strength of the sample first decreased and then increased due to the increase in layer thickness. The main reason for the decrease in the strength is the interlayer bonding which deteriorates on the application of higher temperature. Once the layer thickness increases to a certain level the effect of temperature minimizes and the tensile strength starts increasing. Similarly, the tensile strength increases with the higher raster angle, because the higher angle produces a small raster, hence causing less deterioration. It is also observed that the decrease in space between the layers due to larger air gap also improves the tensile strength of the sample because the positive air gap provides a high amount of heat dissipation thus improving the strength.

Bagsik *et al*. conducted a tensile test at a specific temperature of 230° C to investigate the strength of specimen with different orientations [12]. The result showed that the specimen built in

the direction of X-axis showed maximum strength whereas the sample built in Z-axis showed the least value of tensile strength. The microscopic analysis showed that the bonding between the layers in a specimen built in the Z-direction is not strong enough to resist the loading, hence showing a lower value of tensile strength. He also concluded that the effective cross- sectional area of the sample built in the Z-direction is smaller, due to which the tensile strength decreased.

Sood *et al.* analyzed the change in specimen dimensions over the application oftemperature [24]. It was noticed that with the application of temperature the process of shrinkage was predominant in the width and length direction and the dimensions increased over the thickness. The shrinkage process is due to the stress generated due to the application of temperature, resulting in contraction of fibres. However, it was also observed that once the temperature passes to the glass transition temperature and cooling of the fibres, the uneven temperature gradient results in accumulation of heat stress which decreases the range of tensile load.

Giordano *et al*. analyzed the infill pattern with the layer thickness and print performance [25]. The study explains that a filament with a thicker diameter provides better mechanical properties with the build orientation in X and Y plane. However, a thin filament shows higher tensile strength at building in the Z-direction. This also explains that with higher infill density a higher value of strength is endured until it reaches a point where infill density does not have a significant effect on tensile strength of the sample.

Luzanin *et al.* examined the influence of layer thickness, deposition angle and infill density on the flexural strength of the specimen produced by polylactic acid (PLA) [26]. The range of infill density used was from 10 % to 30 %. The experimental results showed that the layer thickness has a dominant and significant effect on the flexural strength of the PLA specimen, whereas the deposition angle and infill showed no effect on the flexural strength. He also concluded that layer thickness is the major contributing factor for computing the flexural strength of the sample. The results showed that with the increase in layer thickness the value of flexural strength changes from a higher to a lower value which is approximately three times smaller.

The experimental data also revealed that the infill density and deposition angle are dependent variables. The change in deposition angle indicates a larger effect when infill density is low.

The further studies illustrated that the flexural strength yields are at a maximum when deposition angle and infill density lie near the points of 10% and 60 ^{o}, respectively.

Antonio *et al.* studied the experimental characterization of PLA-fabricated parts [27]. He examined the tensile strength of the sample by changing the number of contours, layer thickness and build orientation. The results illustrated that due to anisotropic behavior, the fabricated parts are highly sensitive to the parameters used during processing. The ultimate tensile strength of the material is highly related to the infill orientation and the number of contours. As the infill orientation decreases the strength of the produced part decreases with the increase in layer thickness. This revealed that on increasing the number of the contours the fibre oriented in the longitudinal direction can withstand higher load.

He also concluded that tensile strength showed higher value with a larger number of contours and greater layer thickness. However, the lower value of tensile strength is the function of bonding between the fibre surface and the air gap. The study on elastic modulus showed that the maximum value is attained at the minimum value of infill orientation, and the maximum number of contours, which is due to the fibres that are oriented along the line in which parts are loaded. He also describes that a microscopic view of surface fracture showed that the ductile failure of the specimen occurs when the fibres are pulled until the yield point where the material separates from the plane which is normal to the direction of the force.

Gordon *et al*. demonstrated that the specimen constructed with an increasing number of contours have a higher range of tensile strength [28]. This is because all fibres are aligned in an orientation along the axis of force applied. With the increasing number of contours, the load is distributed and resisted by the line of contour rather than breaking the bond between the layers. It can be concluded that the rectilinear infill pattern shows the highest tensile strength. It is clear that infill density raster angle and build orientation are the most influential factors as far as tensile strength of the specimen is a concern. The tensile strength of the material is also affected by the chain alignment of the filament. The filament material extruded from the nozzle is also influenced by the functional group, the side chain and the chain orientation. Due to high environmental consideration biodegradable polymers such as polylactic acid are some of the most emerging polymers used in 3 D printers.

Research methodology

Mechanical characteristics, specifically the

tensile property is one of the basic parameters that need to br determined when dealing with FDM-processed parts. To perform the tensile test, a number of parameters are considered to get a logical and rational result. Due to the anisotropic properties of FDM parts, it is difficult to predict the results using linear mathematical models. From the literature review it is evident that every adjacent layer fabricated by FDM technique possesses a different property, hence the overall sample shows a nonlinear behavior. To overcome this problem curves using higher polynomial are constructed. The published literature shows that tensile strength can be influenced by the raster orientation and the number of contours while keeping other parameters constant. It is also observed that tensile strength can be affected by infill density till a certain point after which there is very less effect of infill density over tensile strength. So a mathematical model is calculated to determine the tensile strength of sample specimen that are manufactured using modified ASTM D638, in which the orientation of the model varies from 0 ^{o,} to 45 ^{o}, and the number of the contours is 2, 3 and 4, keeping infill density at 25%.

Polylactic acid (PLA) is one of the most commonly used FDM materials after ABS. So a filament of PLA material of diameter 3.0 mm was used to fabricate specimen. The tensile strength of the feed sample was found to be 29 MPa. A Prusa Mendel i3 was used to prepare the samples. Considering the experimental setup used by Antonio *et al.*, the run sample was made according to the modified ASTM D638 type 1 standard. In Figure 13 the dog bone sample is the most commonly used specimen shape to determine tensile strength [27].

The Zwick/Roell ProLine table-top testing Z005 machine was employed for the destructive tensile testing of 54 samples with different combinations. The machine has its software, third generation test Xpert II testing software. The machine works on the manually gripping flat-jaws system, and automatically switches to the eco mode when not in use. The test was carried out at a rate of 2.4 mm/min. The machine has its database system where the data of each sample are saved.

RESULTS AND DISCUSSION

Samples were manufactured using the methodology discussed. Three samples of each parameter were made in order to minimize error and get the best possible results. Samples were tested destructively as mentioned in the methodology. The experimental data of all samples are given in Tables 1 and 2. There are two variables considered; the variation of tensile strength concerning orientation and contour and second stress-strain analysis at constant raster angle.

The variation of tensile strength with respect to the orientation

Figure 14 shows the results of the tensile strength of different samples built at raster angle 0 ^{o}, 15 ^{o}, 30 ^{o}, and 45 ^{o}. Besides that two different infill patterns - concentric and honey comb structures - were also considered to study the tensile strength of the PLA sample. Fig. 14 depicts all trends of raster angle and tensile strength superimposed on the same plot.

Figure 15 depicts all trends of infill pattern (concentric and honey comb) superimposed on the same plot. It can be inferred from Figures 14, 15 and 16 that the change in raster angle causes significant variation in the tensile strength. With the increase in raster angle, the tensile strength increases with a specific number of contour and infill density of 25 %. The tensile strength of the infill concentric pattern shows the highest strength with a maximum number of contours. The infill pattern highly influences the tensile strength of the sample manufactured.

The trend of tensile strength with respect to raster angle at a constant contour number 2 is shown in Figure 17. The graph depicts that the increase in build orientation from 0^{o} to 30^{o} results in an increase in tensile strength of the sample, however, when the material is made with the build orientation of 45^{o} the tensile strength decreases. This phenomenon was thoroughly studied by Es-Said who observed the microscopic structure of the sample and determined that at 0^{o} the filaments align themselves in the line of applied force.

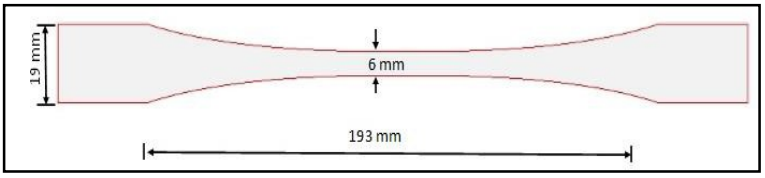

Fig. 13. ASTM D638 modified type 1 specimen [27].

Table 1. Tensile strength of the specimen

Raster angle		No. of contours		
		2	3	4
0^o/-90^o	I	20.7	28.1	62.7
	II	26.5	29.3	33.7
	III	25.3	30.6	25
15^o/-75^o	I	25.5	31	33.4
	II	24.6	33.3	37
	III	25.3	27.2	34.6
30^o/-60^o	I	28.1	34.6	31.5
	II	29.5	34.1	37.8
	III	26.2	32.2	38.8
45^o/-45^o	I	28.9	27.9	38.5
	II	24	33.2	37.5
	III	30.2	32.7	37.5
Concentric	I	25	34.6	39.9
	II	28.9	35.7	39.3
	III	29.2	35	39.7
Honey comb	I	21	30.6	36.1
	II	25.4	30.8	32.8
	III	24.2	28.3	34.9

Table 2. Average data

Raster angle	No. of contours		
	2	3	4
15^o/-75^o	25.13	30.50	35.00
30^o/-60^o	27.93	33.63	36.03
45^o/-45^o	27.70	31.27	37.83
Concentric	27.70	35.10	39.63
Honey comb	29.90	34.60	23.53

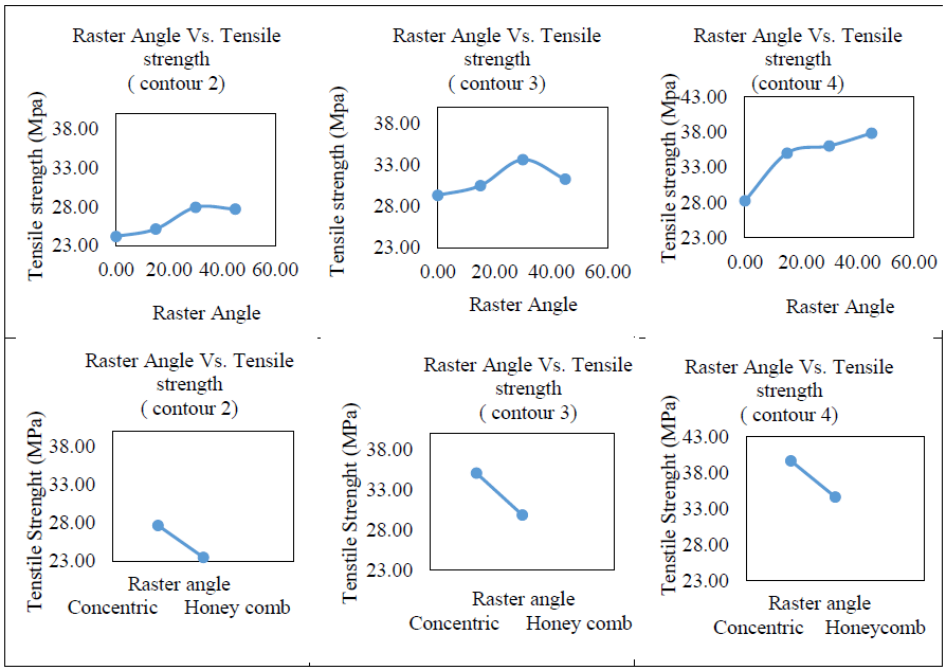

Fig. 14. Strength trends of number of contours 2, 3 and 4

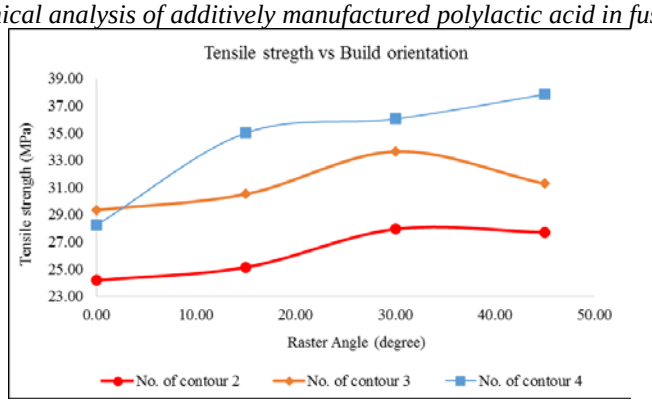

Fig. 15. Trends of contours superimposed

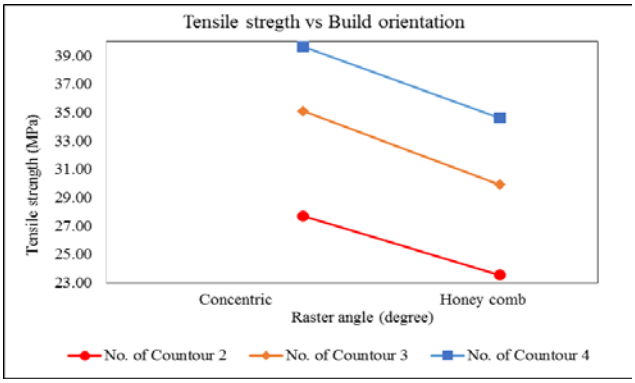

Fig. 16. Trends of all constant densities superimposed with build pattern concentric and honey comb

Number of contours 2 trend

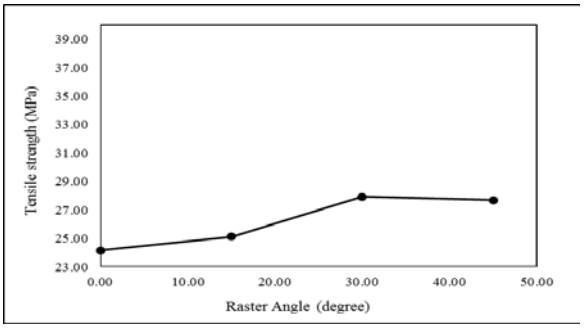

Fig. 17. The trend of tensile strength with respect to raster angle

The trend of tensile strength with respect to raster angle at a constant contour 2 is shown in Figure 17. The graph depicts that with the increase in build orientation from 0º to 30 º results in an increase in tensile strength of the sample, however, when the material made with the build orientation of 45 º the tensile strength decreases. This phenomenon was thoroughly studied Es-Said in which he studies the microscopic structure of the sample determine that at 0 º the filaments align themselves in the line of applied force. It is also observed that at orientation 15 º and 30 º, the higher tensile strength is due to the high alignment of the filament, but reaching at angle 45 º the transverse (90 º) filament is more prominent, so the tensile strength decreases [20]. Figure 18 shows the sample concentric pattern with a number of contours 2.

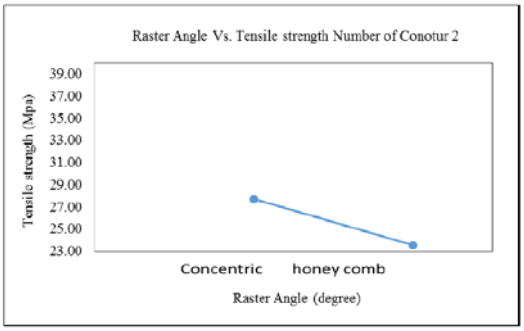

Fig. 18. The trend of tensile strength with a number of contours 2.

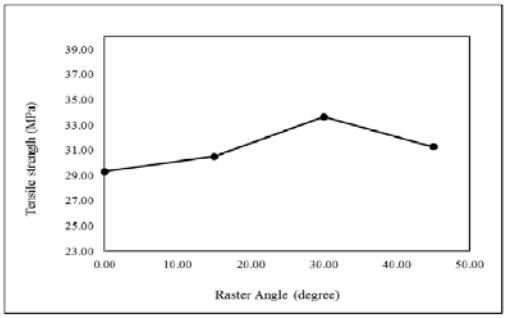

Fig. 19. The trend of tensile strength with respect to raster angle.

Number of contours 3 trend

When the trend of tensile strength is drawn over the contour length of 3, the trend is same as it is for the tensile strength of a number of contour 2 as shown in Figure 19.

However, there lies an anomaly that shows that at 45 º the tensile strength of the sample decreases, the reason of this decrease in tensile strength could be that in build orientation of 45º, delamination phenomenon is more prominent to the tensile load that could be beared by the axially oriented filament, hence, there is a decrease in tensile strength of the sample. Figure 20 shows the trend of tensile strength with a number of contours 3; the trend is the same as it was for 2 contours. The tensile strength is greater for the concentric pattern as it decreases for honey comb infill pattern.

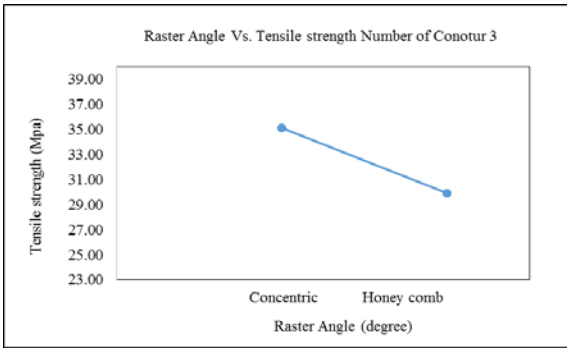

Fig. 20. The trend of tensile strength with a number of contours 3

Number of contours 4 trend

The trend of tensile strength with a contour number of 4 is shown in Figure 21. The strength of the sample increases with the increase in build orientation at a constant number of contours 4. This shows that with the number of contours 4 the tensile strength increases from 0º to 15º due to chain alignment of polymer filament.

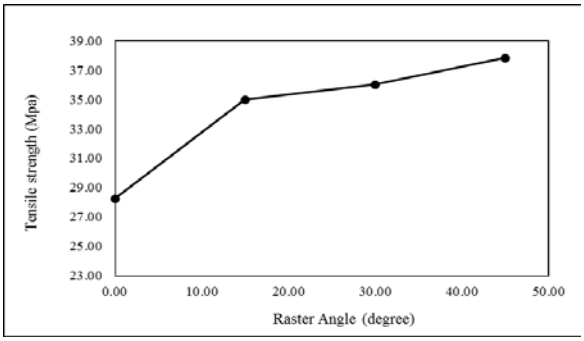

Fig. 21. The trend of tensile strength with respect to raster angle.

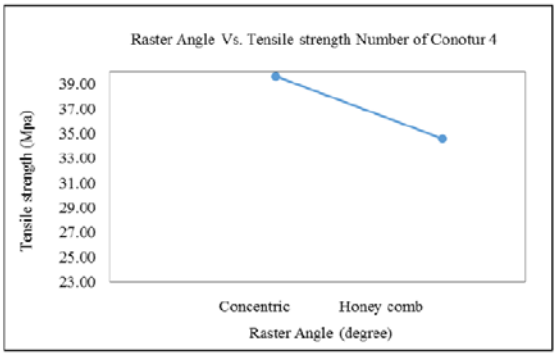

Fig. 22. The trend of tensile strength with a number of contours 4.

The trend pattern for 45º shows that with the increase in the number of contours the tensile strength increases. This is due to the fact that at 45 º and number of contours 4 the load distribution is due to the contour since the filaments are arranged parallel to the direction of load. The axial 0 º is prominent, hence the tensile strength increases [20].

It was found that the tensile strength of the concentric and honey comb structures is higher for concentric structure over honey comb as shown in Figure 22.

The tensile strength analysis of concentric and honey comb structures shows that with a number of contours 2, 3 and 4 concentric pattern shows higher strength as compared to honey comb structure. Figure 23 shows that in the concentric pattern filaments are along the direction of force, however in the concentric pattern the filaments are aligned in the direction perpendicular to the applied force, hence showing less tensile strength.

Fig. 23. Samples with honey comb and concentric pattern.

Variation of tensile strength with respect to the contour

The trend of tensile strength with respect to the number of contours is shown in Figure 24. The trend of strength increases with increasing the number of contours with a specific raster angle.

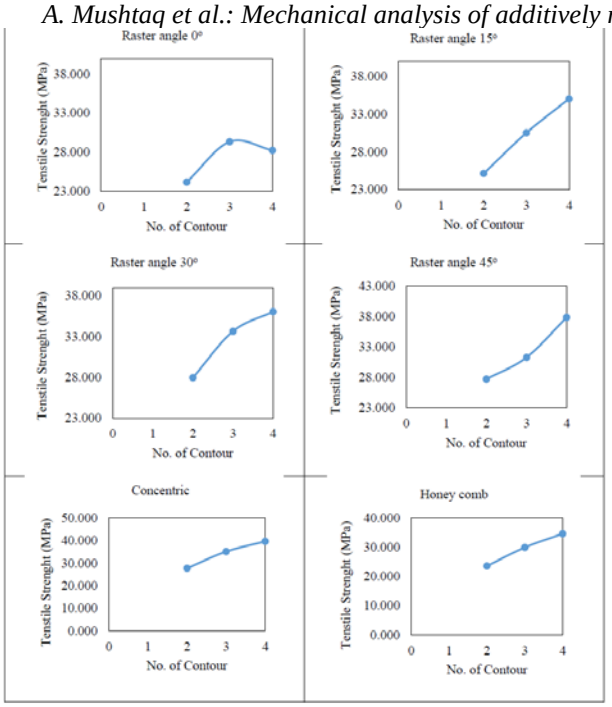

Fig. 24. The trend of tensile strength with build orientation 0º, 15 º, 30 º 45 º, concentric and honey comb

Figure 25 shows the superimposed results of all samples built with raster angle 0 º to 45 º with contour numbers 2, 3 and 4.

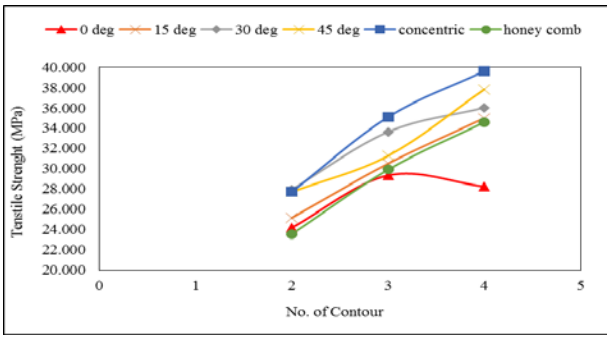

Fig. 25. The trend of tensile strength with build orientation 0^{o},15^{o}, 30^{o}, 45^{o}, concentric and honey comb

0/-90 Degrees trend

Figure 26 shows that as the number of contours increases from 2 to 3 the tensile strength increases with a build orientation of 0º. However, when a sample of 4 contours at 0 º is analyzed, it shows a decrease in tensile strength of the sample.

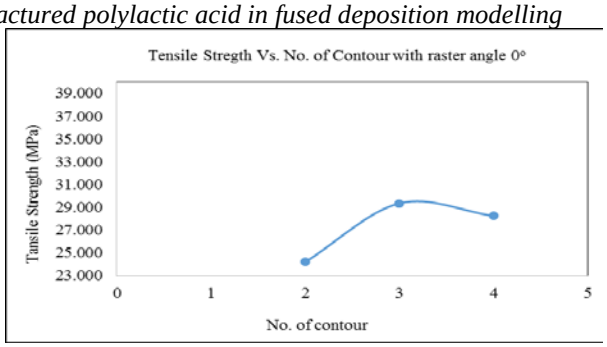

Fig. 26. The trend of tensile strength at 0^{o}/-90^{o}

15/-75 Degrees trend

Figure 27 shows the increase in tensile strength with increase in the number of contours because more filaments are aligned in the direction of the applied force increasing strength.

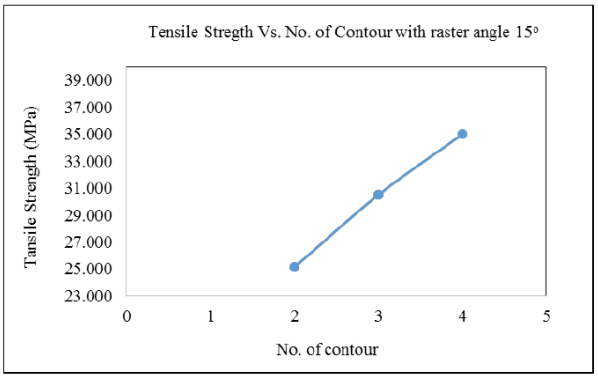

Fig. 27. The trend of tensile strength at 15^{o}/-75^{o}

30/-60 Degrees trend

The plot in Figure 28 shows the strength trend with an increase in the number of contours.

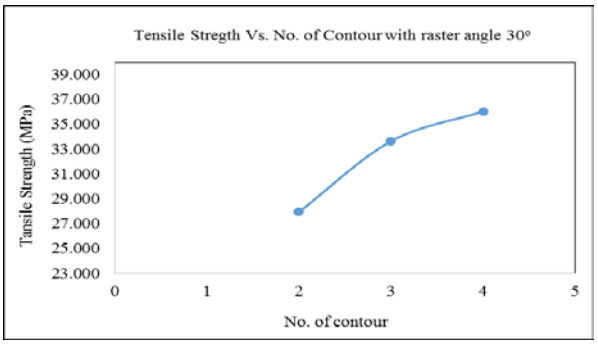

Fig. 28. The trend of tensile strength at 30^{o}/-60^{o}

45/-45 Degrees Trend

A similar trend is observed in tensile strength with increase in contour as compared to building orientation of 0 º, 15 º and 30 º as shown in Figure 29.

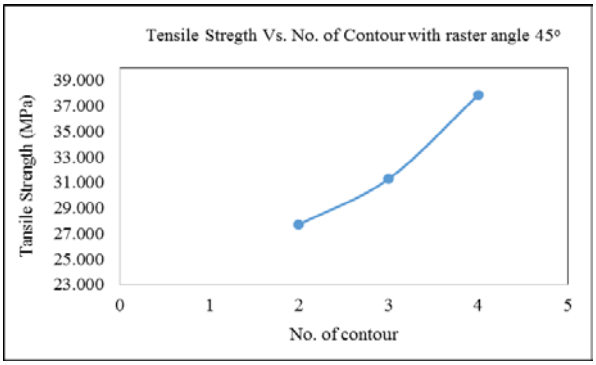

Fig. 29. The trend of tensile strength at 45^{o}/-45^{o}

Concentric pattern

The concentric pattern plot in Figure 30 shows that the pattern has the highest strength among all the samples studied. It is due to the infill pattern showing that maximum filaments during processing are aligned in the direction of applied force, hence, more load can be applied to the sample.

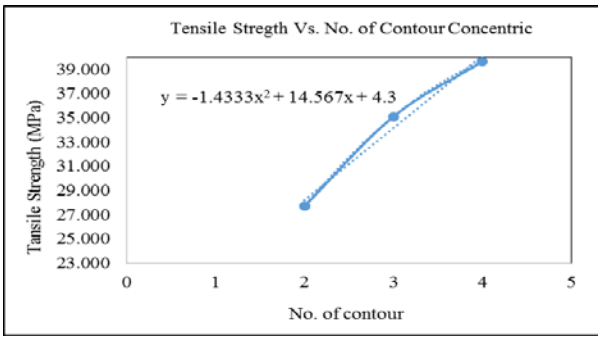

Fig. 30. The trend of tensile strength with a concentric pattern.

Honey Comb

The honey comb structure has a strength that lies in the range of 23 MPa to 35Mpa as shown in Figure 31. This is because in the honey comb structure the infill density can be
the influential factor. The less the infill density, the structure will be the more spacious resulting in bigger voids. These voids would provide a weak point from where the sample can break resulting in lower tensile strength [14, 29].

Stress-strain analysis at constant raster angle

Stress-strain curve basically determines the change in length of the sample due to the application of load. The following trends were observed with the change on contours keeping raster angle constant [30].

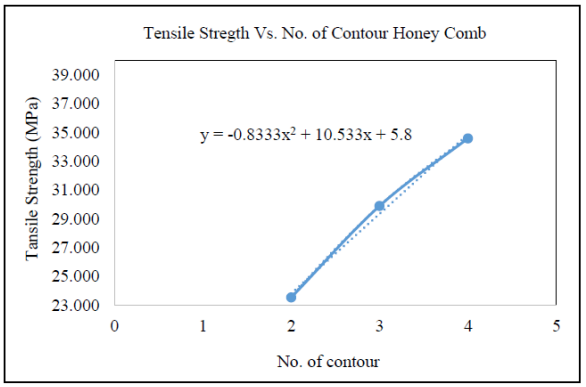

Fig. 31. The trend of tensile strength with honey comb pattern

Stress-strain curve with raster angle 0 °

Figure 32 shows that the sample built with a number of contours 2 has withstood the highest load. Moreover, the sample built with a number of contours 3 has the least value of force tolerated. Similarly, the maximum elongation was experienced in the sample with 4 contours.

Stress-strain curve with raster angle 15 °

It is observed in Figure 33 that with the increase in the number of contours at constant raster angle of 15° the sample could bear a higher force and could experience a stronger elongation.

Stress-strain curve with raster angle 30 °

A similar trend was witnessed in the sample with constant raster angle of 30 ° as was observed in the part built with raster angle 15 °, that with an increase in the number of contours there is an increase in load-bearing capacity of the sample and higher elongation is possible, see Figure 34.

Stress-strain curve with raster angle 45 °

The change in elongation and is more prominent as the number of contour increase as shown in Figure 35. Similarly, the applied force noticeablyincreases with the number of contours.

Stress-strain curve with a concentric pattern

The analysis of the stress-stain curve of the concentric pattern (Figure 36) shows that initially at certain strain the sample with 2 contours have the tendency to tolerate more force, however, reaching a certain strain the sample with 3 contours can endure more force.

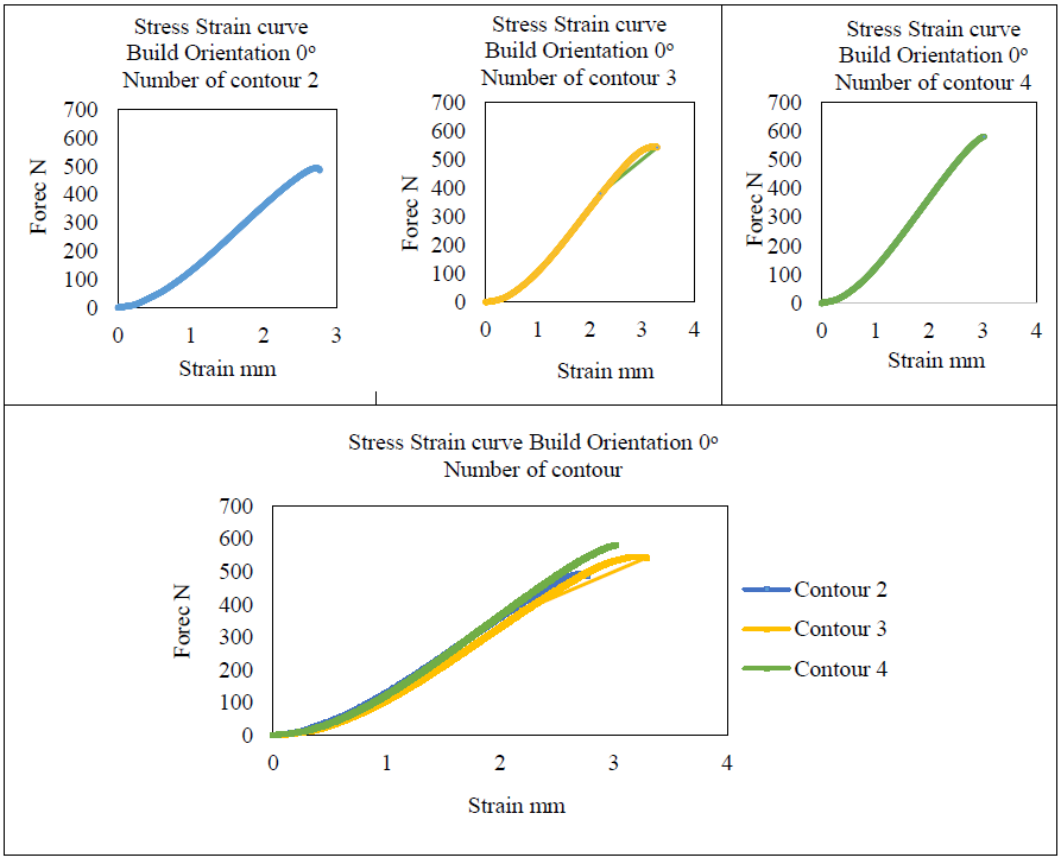

Fig. 32. Stress-strain curve at raster angle 0 °

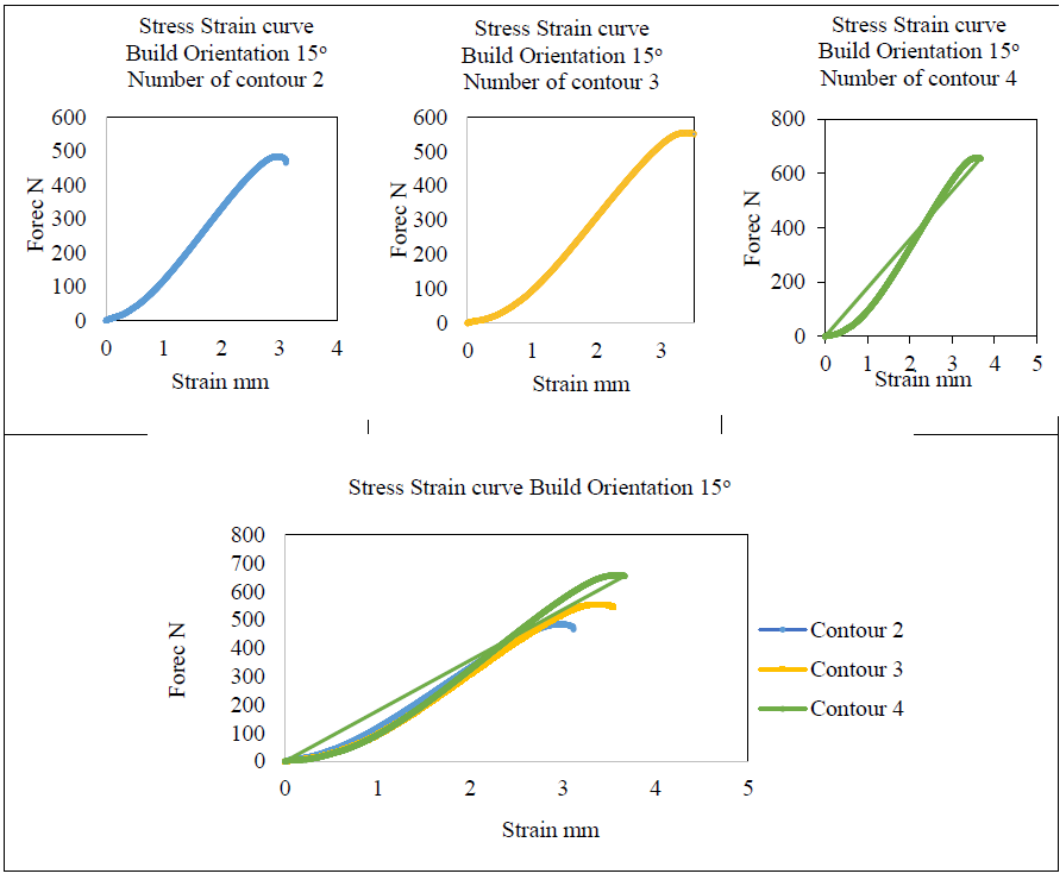

Fig. 33. Stress-strain curve at raster angle15 °

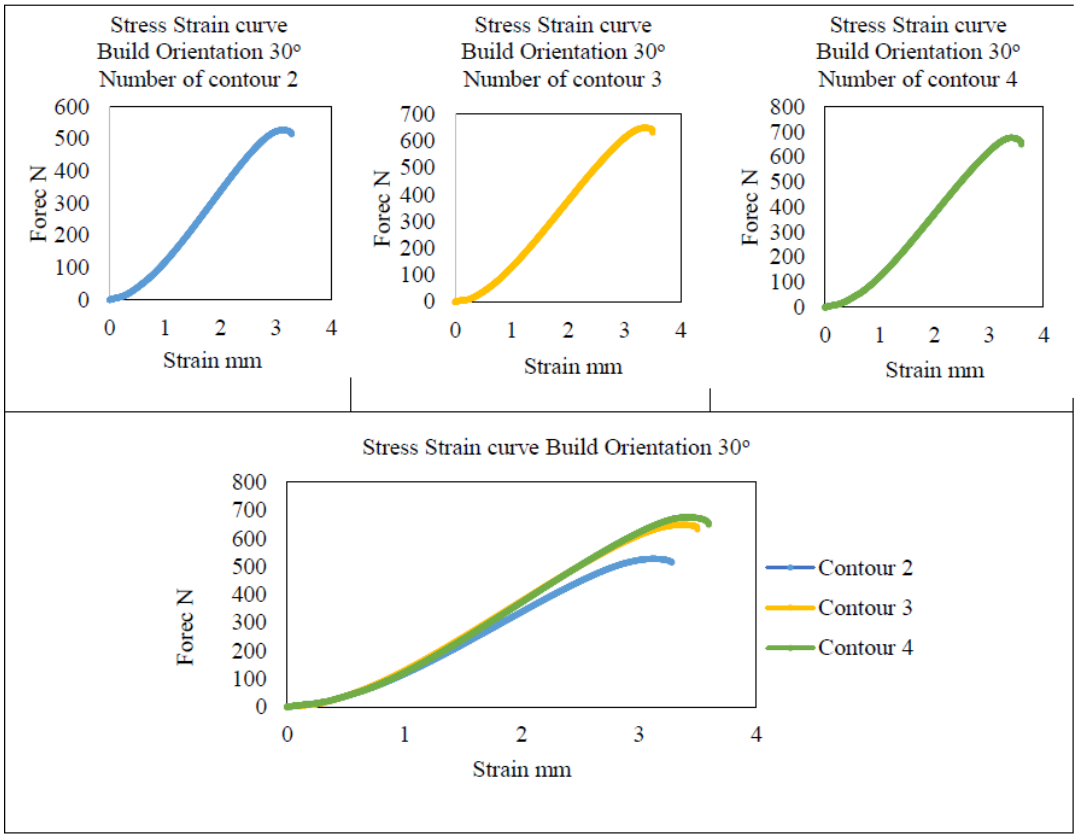

Fig. 34. Stress-strain curve at raster angle 30 °

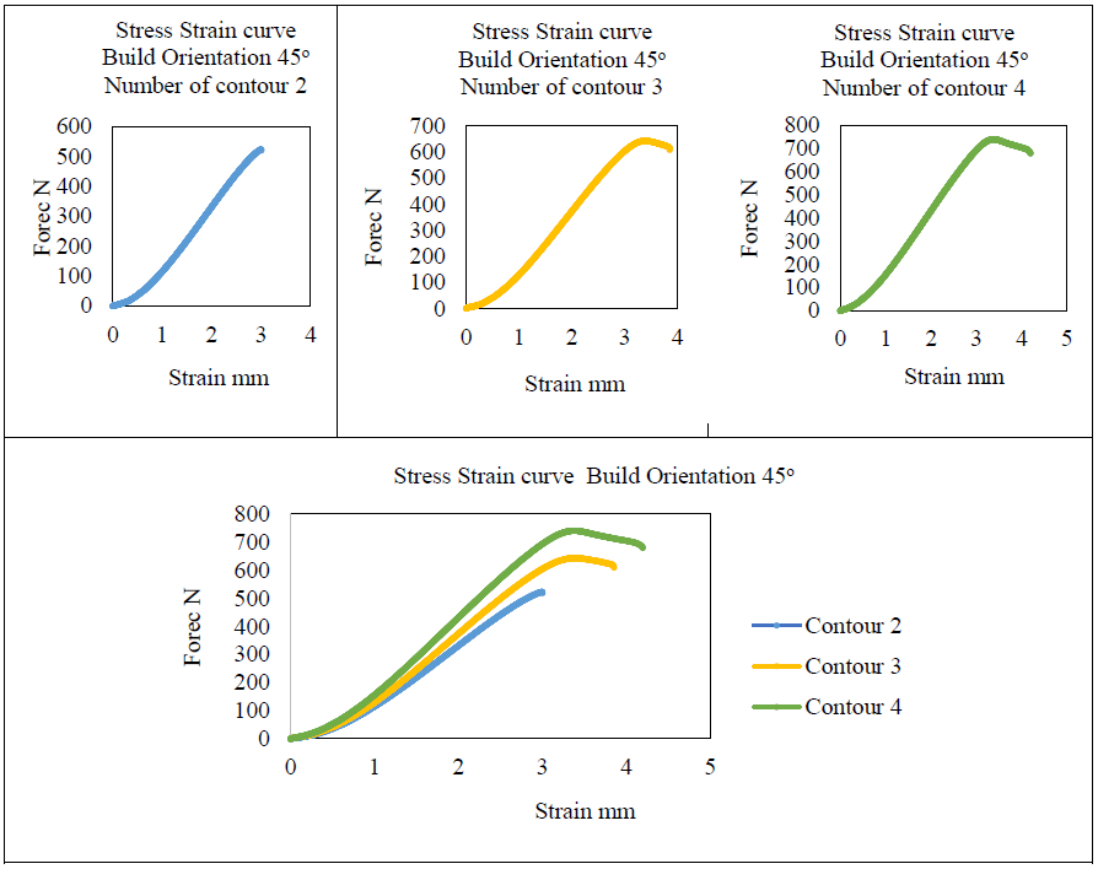

Fig. 35. Stress-strain curve at raster angle 45 °

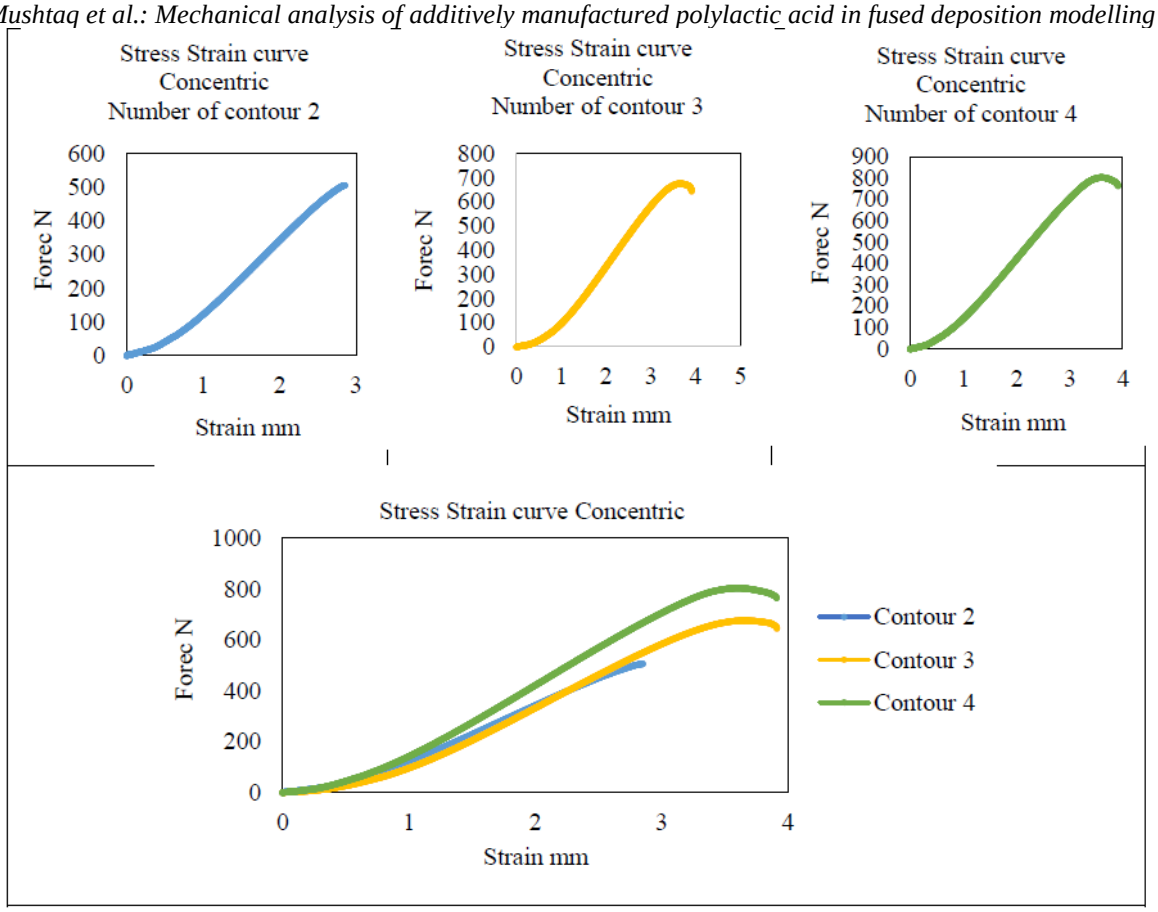

Fig. 36. Stress-strain curve of the concentric pattern

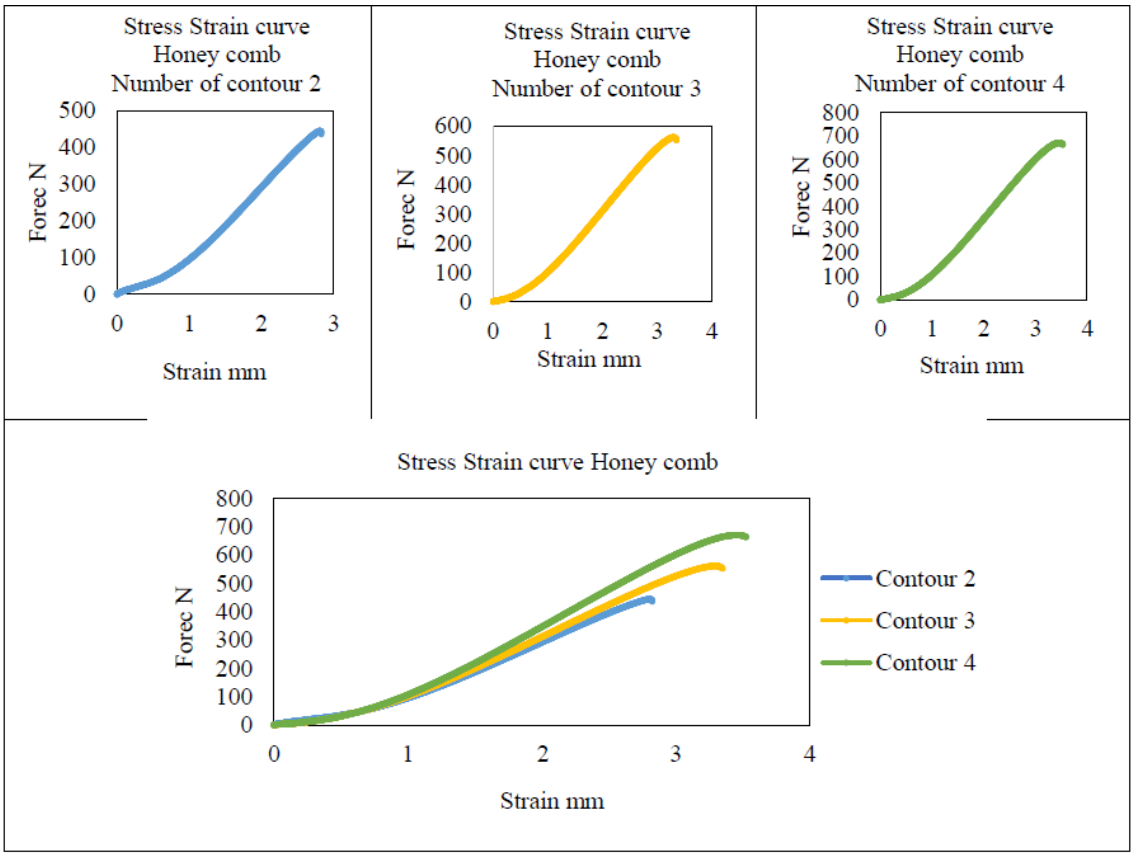

Fig. 37. Stress-strain curve of honey comb pattern

Stress-strain curve with Honey comb pattern

Figure 37 portrays the trend raster angle and different infill patterns are found to be related. In the infill pattern of honey comb the elongation and applied force increases with the number of contours.

The following three mathematical models were established, each for a different raster angle:

1. *TS* /Contours 2= $y = -0.0002x^3 + 0.0149x^2 - 0.1048x + 24.167$

2. *TS*/ Contours 3= $y = -0.0004x^3 + 0.021x^2 - 0.1537x + 29.333$

3. *TS*/ Contours 4 = $y = 0.0003x^3 - 0.0272x^2 + 0.7867x + 28.233$

where x is the raster angle $0^{o} <= x <= 45^{o}$

The following three mathematical models were established, with two different patterns: concentric and honey comb.

TS/Concentric= $y = -1.4333x^2 + 14.567x + 4.3$

TS/Honey Comb= $y = -0.8333x^2 + 10.533x + 5.8$

where x is the number of contours $2<= x <= 4$

With the mathematical models for four different raster angles, there is a better understanding of how the FDM-manufactured objects of PLA material would behave under loading. The tensile strength equation could help to determine the tensile property of polylactic acid having different raster angle and build orientation.

CONCLUSION

The independent study project focused on the tensile strength of a sample by changing the process parameters. After a thorough review of the published literature it was concluded that raster angle and number of contours were the most important parameters to determine the tensile strength of manufactured parts. An open source Fused Deposition Modelling (FDM) machine with a custom-built variation was used in this ISP. The literature review showed that the tensile strength of the polylactic acid manufactured part using different build orientation with different raster angle at constant infill density needs to be determined. The results of this ISP depict that the parts built with concentric pattern show the highest tensile strength with a number of contours 2, 3 and 4. It can also be concluded that with an increase in the number of contours the tensile strength of the PLA sample increases with certain build orientation. The results also show that with an increase in build orientation from 0^{o} to 45^{o} there is an increase in tensile strength of the built sample. This study addressed the need for a mathematical model to correlate the two process parameters, build orientation and raster angle with tensile strength along the layers.

Acknowledgement: *The authors would like to acknowledge the Department of Polymer and Petrochemical Engineering, NED University of Engineering & Technology, Karachi, Pakistan for supporting this research work.*

REFERENCES

1. Y. Huang, M. C. Leu, Report of NSF Additive Manufacturing Workshop, University of Florida, Gainesville, 2014, p. 1.
2. Bártolo, P. Jorge, I. Gibson, History of stereolithographic processes, in: Stereolithography, Springer, Boston, 2011, p. 37.
3. B. C. Gross, J. L. Erkal, S. Y. Lockwood, C. Chen, D. M. Spence, *Anal. Chem.*, **86**, 3240 (2014).
4. C. W. Hull (ed.), in: D.U.S.P.a.T. Office, U.S, 1986.
5. L. Novakova-Marcincinova, I. Kuric, *Manuf. and Ind. Eng.*, **11**, 24 (2012).
6. K. Serguei, E. Boillat, R. Glardon, P. Fischer, M. Locher, *Int. J. Mach. Tool Manuf.*, **44**, 117 (2004).
7. S. Bhandari, B. Regina, *Int. J. Comp. Sci. Inf. Tech. Res.*, **2**, 378 (2014).
8. H. J. Jeea, E. Sachsb, *Adv. Eng. Softw.*, **31**, 97 (2000).
9. J. G. Zhou, D. Herscovici, C. C. Chen, *Int. J. Mach. Tool Manu.*, **40**, 362 (2000).
10. Ferrara, M. Herbert, International directory of company histories, in: J. P. Pederson (ed.) International directory of company histories, St. James Press, 2007.
11. Z. Moza, K. Kitsakis, J. Kechagias, N. Mastorakis, in: 14th International Conference on Instrumentation, Measurement, Circuits and Systems, Salerno, Italy, 2015.
12. A. Bagsik, V. Schöppner, *ANTEC*, **1**, 1 (2011).
13. A. Bagsik, V. Schöppner, E. Klemp, *Polymeric Materials*, **15**, 307 (2010).
14. F. Carrasco, P. Pagès, J. Gámez-Pérez, O. O. Santana, M. L. Maspoch, *Polym. Degrad. Stab.*, **95**, 116 (2010).
15. J. F. Rodriguez, J. P. Thomas, J. E. Renaud., *Rapid Prototyping J.*, **6**, 175 (2000).
16. H.a.S. Executive, Controlling fume during plastics processing, The Health and Safety Executive, U.K, 2013, p. 1.
17. A. K. Sood, R. K. Ohdar, S. S. Mahapatra, *Mater. Des.*, **31**, 287 (2010).
18. S. H. Ahn, M. Montero, D. Odell, S. Roundy, P. K. Wright, *Rapid Prototyping J.*, **8**, 248 (2002).
19. J. Cantrell, S. Rohde, D. Damiani, R. Gurnani, L. DiSandro, J. Anton, A. Young, A. Jerez, D. Steinbach, C. Kroese, P. Ifju, *Rapid Prototyping J.*, **23**, 811 (2017).
20. O. S. Es-Said, J. Foyos, R. Noorani, M. Mendelson, R. Marloth, B. A. Pregger, *Mater. Manuf. Process*, **15**, 107 (2000).
21. M. Montero, S. Roundy, D. Odell, S.-H. Ahn, P. K.

Wright, *Soc. Manuf. Eng.*, **10**, 1 (2001).
22. Q. Sun, G. M. Rizvi, C. T. Bellehumeur, P. Gu, *Rapid Prototyping J.*, **14**, 72 (2008).
23. V. Vega, J. Clements, T. Lam, A. Abad, B. Fritz, N. Ula, O. S. Es-Said, *J. Mater. Eng. Perform.*, **20**, 978 (2010).
24. A. K. Sood, R. K. Ohdar, S. S. Mahapatra, *J. Adv. Res.*, **3**, 81 (2012).
25. R. A. Giordano, B. M. Wu, S. W. Borland, L. G. Cima, E. M. Sachs, M. J. Cima, *J. Biomater. Sci., Polym. Ed.*, **8**, 63 (1997).
26. O. Lužanin, D. Movrin, M. Plančak, *J. Technol. Plast.*, **39**, 49 (2014).
27. A. Lanzotti, D. Eujin Pei, M. Grasso, G. Staiano, M. Martorelli, *Rapid Prototyping J.*, **21**, 604 (2015).
28. E. Fodran, M. Koch, U. Menon, *In Solid Freeform Fab. Proc.*, **1**, 419 (1996).
29. A. Asaa, S. Abazary, A. Masomi, *Int. J. Curr. Eng. Tech.*, **3**, 81 (2013).
30. W. Wu, P. Geng, G. Li, D. Zhao, H. Zhang, J. Zhao, *Materials*, **8**, 5834 (2015).